ELSEVIER

Chemical Engineering Journal 68 (1997) 131–138

Chemical Engineering Journal

Changes in fluid residence time distribution during deep-bed filtration

E. Rodier [a,*], J.A. Dodds [b], D. Leclerc [a], G. Clément [c]

[a] *Laboratoire des Sciences du Génie Chimique, CNRS-ENSIC, 1 rue Grandville, BP 451, 54001 Nancy, France*

[b] *Ecole des Mines d'Albi, Campus Jarlard, 81013 Albi, France*

[c] *Centre de Recherche de Voreppe, Pechiney, BP 27, 38340 Voreppe, France*

Received 3 March 1996; revised 21 May 1997; accepted 6 June 1997

Abstract

An experimental study is presented of the changes in residence time distribution in a granular bed during the course of deep-bed filtration. The results are described in terms of the distribution moments, and show that small amounts of deposit yield large changes in the second moment, with the first moment remaining practically unchanged. Higher moments were calculated, but could not be used because of the large experimental error. Evaluations on the basis of classical models of transport of solutes in porous media attribute these results to the hydrodynamic dispersion changes due to the accumulation of deposits. Interesting results were also obtained by varying the surface conditions of the filter. By turning the wettable glass beads into non-wettable beads the filtration efficiency was significantly enhanced. © 1997 Elsevier Science S.A.

Résumé

On présente une étude expérimentale des changements de distribution de temps de sejour lors de la filtration d'une suspension dans un lit granulaire. Les résultats sont exprimés en termes de moments des distributions et montrent que tandis que le premier moment ne change presque pas, le second moment subit de très grandes variations provoquées par de petites quantités de dépôt seulement. Une analyse basée sur un modèle classique de transport de soluté dans un milieu poreux indique que ces changements pourraient être attribués à l'évolution de la seule dispersion hydrodynamique, évolution due à l'accumulation d'un dépôt dans le filtre. Les moments plus élevés ont aussi été calculés et ils semblent ne pas évoluer durant la filtration. Cependant ils sont peu fiables, l'erreur expérimentale ayant un poids important dans leur calcul. On a d'autre part étudié l'influence de la mouillabilité de la surface du milieu poreux sur la filtration. Il s'avère que l'on a une meilleure efficacité de filtration pour une surface non mouillante que pour une surface mouillante et ceci s'explique par la modification des interactions de surface. © 1997 Elsevier Science S.A.

Keywords: Deep-bed filtration; Fluid residence time distribution; Surface conditions of the filter

1. Introduction

The concept of the residence time distribution (RTD) of a fluid in a reactor was introduced by Danckwerts [1] in chemical engineering and is now widely used in many other domains to interpret how fluids pass through and react in complex flow structures [2]. In this study, we examine how this concept can be applied to industrial processes, such as filtration, where there is a strong coupling between the flow regime and the capture efficiency of the bed.

Deep-bed filtration [3] is a transient process in which particles in suspension flowing through a bed of granular solids are captured at surfaces in the bed. These deposits then change the nature of the capture surfaces and also change the bed structure available for fluid flow. Thus the capture conditions, shown by the filtration efficiency and pressure drop across the bed (at constant flow rate), are interrelated in a complex fashion and change progressively throughout filtration. Theoretical predictions of the evolution of the process have involved model pore shapes and assumptions about the structure of deposits [4]. In situ observations of the changes in bed structure during filtration have also been attempted using an endoscope [5]. The investigation reported here attempts to link changes in filtration efficiency and pressure drop to changes in fluid RTD during the course of filtration. Other workers [6] have made similar measurements and found significant changes in RTD during filtration experiments. In this study, we extend this work using a model filter

* Corresponding author.

PII S1385-8947(97)00073-9

bed composed of glass beads, carefully packed in a liquid chromatographic column, to give good control of the RTD measurements. The technique used involves deep-bed filtration experiments of suspensions of talc particles. At intervals during filtration, impulse injections of market fluid are made at the inlet of the bed and the response curve at the outlet is followed to give the RTD [7]. Preliminary work has confirmed that the KCl tracer gives a linear response and does not interact with the system (glass beads, talc). The experiments show that, whilst the mean residence time remains constant, there are significant changes in the shape of the response curves for very small amounts of particles captured. Three main types of experiment are reported: those involving the first stages of filtration in an initially clean bed, further stages of filtration when the bed starts to become saturated and, finally, examination of the influence of the wettability of the filter medium.

2. Experimental methods

2.1. Experimental equipment

The experimental equipment is shown in Fig. 1. It comprises the following elements:

1. an Ismatec IPN peristaltic pump fitted with Tygon tubes having an inside diameter of 2.29 mm; the maximum flow rate is 5 ml min^{-1} and the maximum counter-pressure is 1.5 bar;
2. a magnetic stirrer;
3. a SenSym SC 100 × DN pressure sensor (0–6 bar; output tension, 5 V);
4. an injection valve with a 350 μl injection loop;
5. a three-way valve placed after the injection valve; it is used to route the flow either through the bypass directly to the detector or via the packed column, thus allowing inlet conditions to be monitored;
6. a Cheminert LC-type glass column containing the packed bed; this column can support a maximum pressure of 5 bar;
7. a Tacussel CDRV 62 conductimeter with 2 V output tension connected to a flow-through conductimetric cell having a constant of 0.5 and a volume of 0.3 ml; the tracer used is potassium chloride (KCl, 0.1 M); in this concentration range, the conductivity varies linearly with the KCl concentration;
8. a PDA 2000 turbidimeter with an output tension of 10 V; in the PDA 2000, the flowing suspension is illuminated by a narrow beam of light so that a fairly small sample volume is examined (of the order of 1 mm^3); the intensity of transmitted light follows the Beer–Lambert law as suspensions are sufficiently dilute; three values are given: the DC component corresponding to the average transmitted light intensity (related to the turbidity of the suspension), the root-mean-square value of the fluctuating signal (RMS) and the ratio between these two values (RMS/DC), which is proportional to the square of the number of particles detected;
9. a computer with an RTI 800/815 board for data acquisition.

All of these elements are linked with Tygon connection tubes.

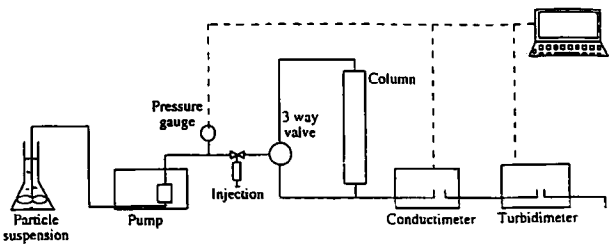

Fig. 1. Experimental set-up.

2.2. Systems used in the experiments

2.2.1. Glass beads

The columns were packed with a sieve cut between 605 and 695 μm of spherical sodo-calcic glass beads having a smooth, non-abrasive and non-porous surface. The beads were thoroughly washed before use in an ultrasonic bath and their density was measured with a Micromeritics helium pycnometer. Streaming current measurements [8] showed that the isoelectric point was close to 2.5 and that the beads were negatively charged at all values of pH above this. Some experiments were performed with glass beads modified by a surface treatment to render them hydrophobic. This was performed by contacting them with a dimethyldichlorosilane solution for 5 min, followed by rinsing with methanol and drying in an oven at 30 °C.

2.2.2. Talc particles

Talc is a magnesium silicate with the formula $Mg_3Si_4O_3(OH)_2$. The particle size distribution was measured with a Malvern Mastersizer light diffraction instrument and was found to have a mean volume diameter of 2 μm with $d_{10} = 1.0$ μm and $d_{90} = 10.9$ μm. The surface/volume mean diameter ($d_{3,2}$) was 5.52 μm. Observations with a scanning electron microscope showed that the particles were roughly tablet shaped. Therefore the mean diameter given above is merely an order of magnitude of the size of the particles.

2.3. Interpretation method of results

2.3.1. Turbidity and pressure

Pressure and turbidity values are reported relative to the inlet conditions. The latter depends on the suspension concentration, and such values are adequate for qualitative appreciation. A HIAC/ROYCO particle counter was used for a more precise evaluation of the particle concentration at the outlet of the column, so as to obtain more accurate mass balances. The flow rate and concentrations employed did not

allow this counter to be used on-line and these measurements were therefore only made at intervals on collected samples.

2.3.2. Determination of RTD [2]

RTD was determined from the impulse response of an inert tracer introduced into the flowing suspension by means of an injection valve. The duration of the injection time with a 350 μl injection loop and an entering flow rate of Q_e is $t_i = 0.350(\text{ml})/Q_e(\text{ml min}^{-1})$.

The RTD function

$$F(t_s) = \int_0^t E(t_s)t_s$$

is defined as the probability that a fluid element has a residence time less than t. $E(t_s)$ is the residence time density function. Statistical moments of this distribution are given by: moment of order n

$$\mu_n = \int_0^\infty t_s^n E(t_s)t_s \quad (1)$$

$\mu_1 = \bar{t_s}$ is the mean residence time of the particles in the column. The order n central moment is defined as

$$\mu'_n = \int_0^\infty (t_s - \bar{t_s})^n E(t_s)t_s \quad (2)$$

Table 1
Experimental parameters

Suspension	Talc particles
	ζ potential < 0
	d_{mean} of particles, 2 μm
	Talc density, 3200 kg m^{-3}
	Suspension concentration, 0.75 g l^{-1}
Porous medium	Column packed with glass beads
	ζ potential < 0
	Column: Cheminert; inside diameter, 2.54 cm; length, 15 cm
	Glass beads: sieve cut, 605–695 μm; density, 2.705 kg m^{-3}
	Porosity of the filter bed, 0.38 (mean value)
Aqueous solution	Solution of KCl, pH non-adjusted
	Ionic strength, 10^{-3} M
	pH (entry of the column), water pH
Flow rate, Q_e	3.15 ml min^{-1} (mean value)
Tracer	Solution of KCl, 1×10^{-1} M
	Injected volume, 350 μl

The second central moment $\mu'_2 = \sigma^2 = \mu_2 - \mu_1^2$ is the variance of the distribution. These moments have been determined from the response curves with points taken every 5 or 10 s and integration taking into account the delay induced by tubing and the reduction of the porous volume if significant. Higher order moments are difficult to interpret owing to their great sensitivity to the tails of the response curves and the consequent large uncertainty in their experimental determination. Such results for the third and the fourth moments only indicate that they do not vary significantly in the experiments reported here.

3. Deep-bed filtration experiments

3.1. Experimental set-up

The experimental parameters are given in Table 1 and the different experiments performed are summarized in Table 2. The experimental method used was as follows.

1. The filter bed was first conditioned by passing through it a solution of the same ionic strength as the talc suspension which was to be filtered.
2. Filtration was then commenced by passing the talc suspension through the filter bed and continuously logging the pressure and turbidity values at the outlet. At intervals during the course of filtration, an impulse of tracer fluid was injected into the bed and the response curve at the outlet was determined by conductivity. These readings were used to determine the RTD.
3. At the end of the experiment, the packing was emptied from the column and thoroughly washed with demineralized water in an ultrasonic bath before re-packing for the next experiment.

All experiments were performed in laminar flow conditions, i.e. the pore Reynolds number (defined as $Re_p = \rho u_m / a_g(1-\epsilon)\eta$) was always less than unity ($Q_e = 3.1$ ml min^{-1}, $\epsilon = 0.38$ and $d_g = 650$ μm, giving $Re_p = 1.78 \times 10^{-2}$).

3.2. Results

The evolution of filtration was followed by measurement of the pressure drop across the column and the solid concentration at the column outlet. The latter was determined using a HIAC/ROYCO particle counter and by turbidity. These values were used to calculate the filtration efficiency, defined as the ratio of the amount of particles captured to the amount

Table 2
Deep-bed filtration experiments (mean values for Q_e and t_f)

Experiment	Filtration time (min)	Pore volume (ml)	State of the filter surface	Q_e (ml min^{-1})
6, 7, 8	480	28.72	Wettable	3.16
16, 17, 18	480	30.26	Non-wettable	3.10
19, 20	600	11.84	Wettable	3.12
21, 22	600	11.65	Non-wettable	3.06

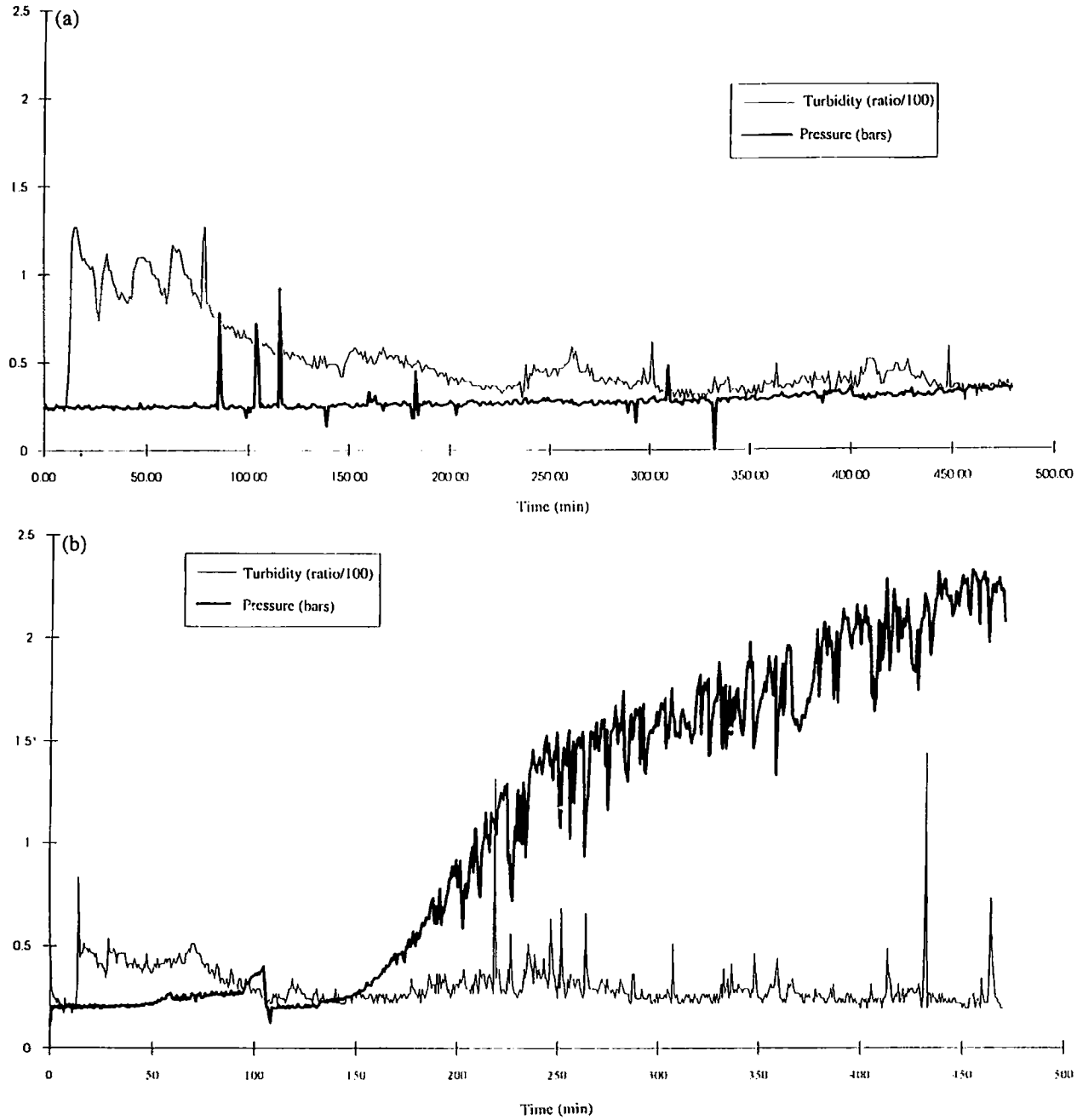

Fig. 2. (a) Pressure and turbidity signals as a function of duration of filtration. (b) Pressure and turbidity signals as a function of duration of filtration.

of particles introduced as a function of time. The impulse response curves were analysed to give the mean residence time, or first moment, the variance of the tracer peaks and higher moments. In some experiments, the packing was left to dry before being pushed piston-like out of the column and sectioned for observation using a scanning electron microscope. Fig. 2(a) shows typical results for the turbidity at the column outlet and the pressure drop. As a contrast, Fig. 2(b) shows the results corresponding to filtration with treated, non-wettable glass beads; in this specific case, there is an additional flocculation phenomenon giving rise to a significant increase in pressure drop during filtration. This will be discussed later. Fig. 3 shows the results in terms of the filtration efficiency for experiments 6, 7, 8 and 16, which can be seen to be roughly constant at around 98%–99%. Fig. 4 shows a typical series of impulse responses during a filtration run using wettable glass beads. The same sort of impulse responses are obtained for non-wettable beads.

It can be seen that the initially clean beds give the expected symmetrical gaussian curve and that, during the course of filtration, the response curves exhibit progressively longer and longer tails. For experiments 6–8 and 16–18, with a 480 min filtration time, the mean residence time remains constant at around one pore volume. This is an expected result since the porous volume is not significantly modified. The talc introduced represents a volume of 0.35 cm^3, i.e. 1.3% of the

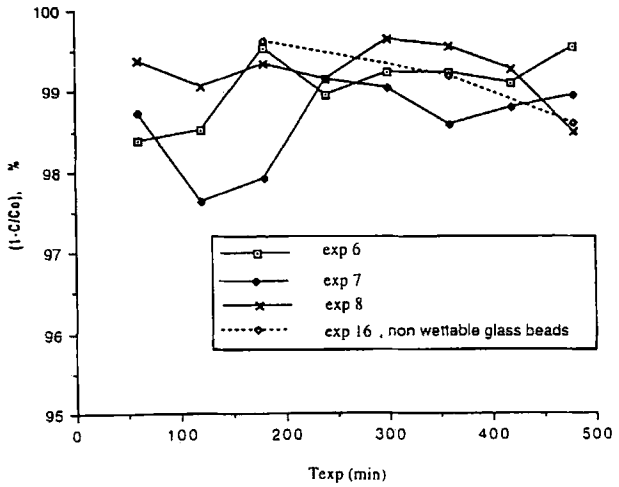

Fig. 3. Filtration efficiency as a function of filtration time for experiments with wettable and non-wettable glass beads.

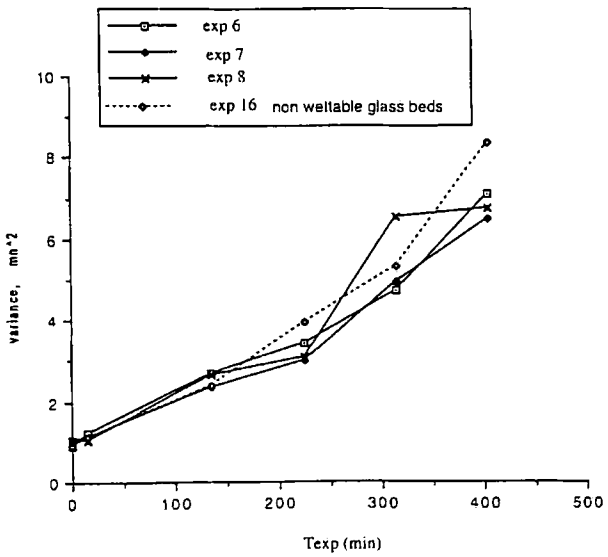

Fig. 5. Variance as a function of duration of filtration.

total pore volume. We can evaluate the amount of talc deposited by the difference between the weight of the bed before the experiment and the weight of the bed after the experiment, having dried the bed before weighing it. The evolution of the variance is shown in Fig. 5.

The variations of the mean residence time (Fig. 6) and the filtration efficiency (Fig. 7) are also shown in the case of a wettable filter bed (experiment 20) and a non-wettable filter bed (experiment 22). Let us consider experiments 19–22 (see Table 2) where a greater degree of saturation of the filter (1.42 g of talc, i.e. 3.77% of the total porous volume) is deposited in the bed. Even in this case, the trends in the RTD results are identical with those discussed above (experiments 6–8 and 16–18), and the first moment is not sensitive to this small variation in pore volume.

3.3. Discussion

Firstly, let us consider the increase in peak dispersion with filtration time. How should the evolution of the shape of the impulse response peaks be interpreted? Both continuous and discrete models [9] have been used to represent solute transport in porous media. These two types of model are equivalent when the Peclet number ($Pe = u_m L/\epsilon D$) is greater than about five or ten. The models assume that the pore volume available for flow, i.e. the void volume between the packing grains, can be divided into zones of immobile fluid and mobile fluid. The convective–dispersive transport of a non-reacting solute (as for our tracer) is assumed to be confined to the mobile phase, whereas solute transfer between mobile and immobile

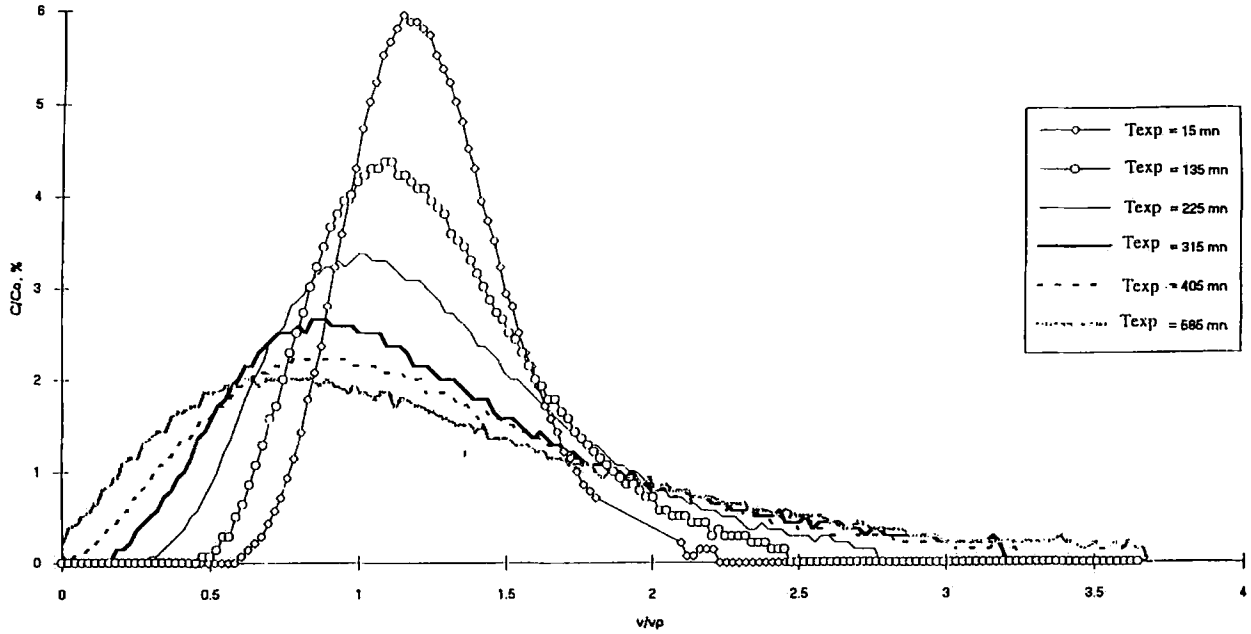

Fig. 4. Residence time distributions as a function of duration of filtration for wettable glass beads.

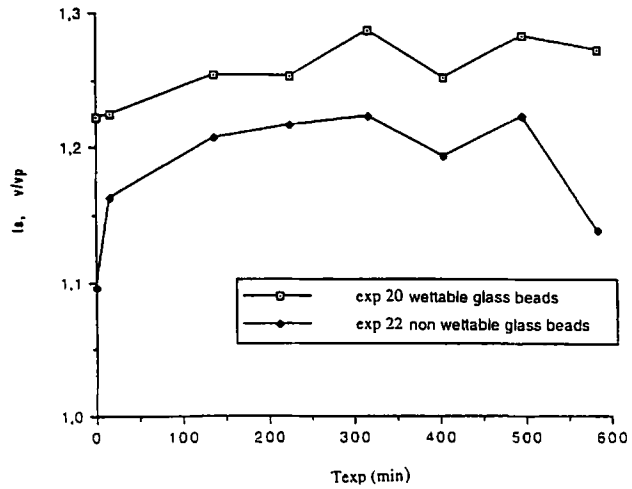

Fig. 6. Mean residence time as a function of duration of filtration for experiments with wettable and non-wettable glass beads.

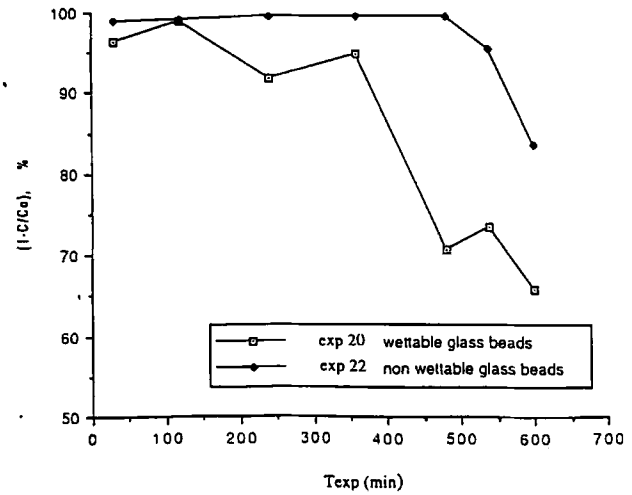

Fig. 7. Filtration efficiency as a function of duration of filtration for experiments with wettable and non-wettable glass beads.

porous media–aqueous suspension is assumed to be diffusion controlled. The discrete parameter model assumes that spatial variations are represented by a series of J connected mixing cells, each having a uniform composition. Each cell has a volume V/J (V is the total porous volume) and contains mobile and immobile water volumes of $\theta_m V/J$ and $\theta_{im} V/J$ respectively. The mass balance equations for the solute are as follows: in the mobile zone ($j = 1, 2, 3, \ldots, J$)

$$Q_e C_{m,j-1} = Q_e C_{m,j} + \frac{\theta_m V}{J}\frac{dC_{m,j}}{dt} + \frac{\theta_{im} V}{J}\frac{dC_{im,j}}{dt} \quad (3)$$

in the immobile zone

$$\theta_{im}\frac{dC_{im,j}}{dt} = k_M(C_{m,j} - C_{im,j}) \quad (4)$$

where $C_{m,j}$ is the solute concentration of the mobile water at the outlet of cell j, $C_{im,j}$ is the associated solute concentration of the immobile water at the outlet of cell j and k_M is the overall mass transfer coefficient.

For each cell, a transfer function can be defined in the Laplace domain, $G_j(s) = \bar{C}_{m,j}/\bar{C}_{m,j-1}$, and hence for the porous medium as a whole

$$G(s) = \bar{C}_{m,J}/\bar{C}_{m,0} = \prod_{j=1}^{J} G_j(s)$$

The RTD moments are obtained from relation (1) expressed in the Laplace domain. Finally, we have

$$t_s = t_m(1 + K_{im}) \quad (5)$$

and the reduced variance of the RTD is such that

$$\sigma'^2 = \frac{\sigma^2}{T_s^2} = \frac{\mu'_2}{T_s^2} = \frac{2}{t_m}(t_D + t'_M) \quad (6)$$

with the following characteristic times defined as

$$t_m = \frac{L\epsilon}{u_m} \text{ convection time in the mobile phase} \quad (7)$$

$$t_D = \frac{t_m}{Pe} \text{ dispersion time} \quad (8)$$

$$t'_M = \frac{K_{im}}{(1 + K_{im})^2} t_M \text{ modified transfer time} \quad (9)$$

where K_{im} is the ratio between the mobile and immobile zones of the porous volume and t_M is the transfer time of the solute between the two zones.

It is assumed that convection prevails at the inlet and outlet boundaries. This discrete model is very general and allows a description of a wide range of flow patterns by making a suitable choice of cell volumes and connections between them. Here it is used to represent the filter bed as a cascade of J identical mixing cells in series.

The evaluation of the characteristic times can be a powerful method for isolating the predominant processes responsible for the shape of the RTD curves. t_m is easily calculated from the experimental conditions. t_D can be calculated using the discrete model described above. The equivalence between discrete and continuous models gives $Pe = 2J$, and J can be determined graphically [2] by considering the first symmetrical part of the RTD peak and ignoring the tail, if there is one. Having σ'^2, t_m and t_D, we can deduce t'_M. The values found are summarized in Table 3.

As long as $t'_M \ll t_D$, hydrodynamic dispersion can be considered to be the predominant process for broadening the RTD. The larger the Peclet number, the more symmetrical the RTD. This case corresponds to the initial part of all the filtration experiments reported here. When $t'_M \approx t_D$, the RTD broadens and loses its symmetrical shape. Immobile zones of fluid begin to become important. This case obtains at the end of the filtration experiments. When $t'_M \gg t_D$, mass transfer between the mobile and immobile regions is the predominant process for broadening the RTD. In this latter case, the RTD becomes quite asymmetrical, but this does not occur in our experiments.

Table 3
Characteristic dispersion and transfer times [9] for the experiments

Experiment	T_{exp} (min)	J	Pe	t_D (min)	t'_M (min)	t_D/t'_M	Conclusion
7	15	100	200	0.046	2.60×10^{-3}	18	$t_D > t'_M$
7	405	40	80	0.114	2.62×10^{-1}	0.43	$t'_M \approx t_D$
17	15	100	200	0.048	4.79×10^{-4}	101	$t_D \gg t'_M$
17	405	70	140	0.070	1.80×10^{-1}	0.39	$t'_M \approx t_D$
20	15	25	50	0.076	2.00×10^{-5}	3790	$t_D \gg t'_M$
20	585	4	8	0.668	3.84×10^{-1}	1.74	$t'_M \approx t_D$
22	15	20	40	0.103	3.07×10^{-4}	335	$t_D \gg t'_M$
22	585	4	8	0.460	2.73×10^{-1}	1.68	$t'_M \approx t_D$

The filtration efficiency is at least 95% at the beginning of filtration (experiments 6–8 and 16–18). It decreases after 300 min in the case of non-treated glass beads (experiment 20) and after 500 min in the case of treated glass beads (experiments 21 and 22). This can be seen in Fig. 7. This indicates that filtration is more efficient in the case of non-wettable glass beads; this must be partly due to hydrophobic interactions encouraging attraction between glass and talc to the detriment of contacts between glass and water molecules.

In all experiments, except 17 and 18, there is only a slight variation in the pressure drop (Fig. 2(a)) over the whole duration of filtration. This is a classic result when the porosity varies only slightly (the decrease in porosity is only 1.24% in experiments 6–8). In normal cases [3], when the retention is low, the pressure drop varies linearly with the filtration time. This is observed, but with a very small slope ($\Delta p/\Delta p_0 = 1 + 7.8\times10^{-4}T_{exp}$). In all the experiments, except 17 and 18, the turbidity (Fig. 2(b)) is directly linked to the filtration efficiency. Any decrease in efficiency results in an increase in turbidity.

Experiment 17 shows turbidity peaks after 3 h of filtration (Fig. 2(b)). These are characteristic of the presence of flocs, indicating that the talc particles have agglomerated. It should be noted that silane treatment was not renewed between experiments and the surface properties may alter during the experiments. In the ideal case, the silane deposit should only influence the interactions between talc and glass beads by strengthening the hydrophobic nature of the porous medium and thus favouring the deposition of talc on the glass beads. However, the presence of talc flocs could be due to surface flocculation and subsequent detachment to be carried off in the flow. The fact that the pressure drop fluctuates in experiment 17 (Fig. 2(b)) and increases from 100 min onwards may be due to pore plugging by the flocs.

Nevertheless, it should be noted that the RTD results are similar for experiments 6–8 and 16–18. For example, at filtration time $T_{exp} = 405$ min, the mean residence times of experiments 7 and 17 are 1.10 and $1.13v/v_p$ respectively and the variances are 6.44 and 6.52 min^2. Whatever the pressure and turbidity evolution, the RTD curves are similar.

Visual and scanning electron microscopy observations made on experiments 6, 7, 8 and 20 show that, at the column inlet, the talc particles are distributed over the whole surface of the glass beads, with the talc deposit being thicker at the points of contact and in cracks in the surfaces of the beads.

4. Conclusions

Deep-bed filtration experiments were performed in a model system in which the particles to be filtered represented at most 4% of the total pore volume of the filter. The filtration efficiency and bed pressure drop measurements were monitored during filtration, as were the changes in the fluid residence time, presented here in terms of the mean residence time and its variance. It was found that, whilst the mean residence time remained roughly constant, the variance varied considerably during the course of filtration. By applying the general model of mixing cells in series [9], the predominant peak broadening process was found to be hydrodynamic dispersion. As the filtration proceeded, the pore size distribution of the porous medium broadened, as did the hydrodynamic dispersion. Small amounts of deposit in the packed bed led to large changes in the impulse response. It can be concluded that small quantities of particles accumulating in locations, such as at contact points between grains, produce large changes in the flow structure in the pore volume.

It was also observed that, whatever the evolution of turbidity and pressure, the RTDs were always similar. It can be concluded that RTD measurements provide information on the changes in the porous structure only and do not reflect the behaviour of bed filters as a whole.

Finally, an interesting result of this study is that the filtration efficiency can be increased greatly by modifying the surface conditions of the filter bed. Treating wettable glass beads to make them non-wettable (in aqueous filtration) influences the interactions between the beads and the particles to be filtered. Non-wettable glass beads induce hydrophobic interactions which are attractive and can act over a long range [10], e.g. 80–100 nm. This is roughly 3% of the particle diameter of the talc used and hence is significant at the particle scale.

Both the variance evolution of the RTD curves and the influence of surface conditions in deep-bed filtration merit further study.

Appendix A. Nomenclature

a_g	specific surface of the packing ($6/d_g$ for spherical grains) (m^{-1})
C	particle concentration of outlet solution (mg l^{-1})
C_0	particle concentration of inlet solution (mg l^{-1})
C_m, C_{im}	concentrations of solute (tracer) in the mobile and immobile water (mg l^{-1})
D	longitudinal dispersion (m^2 s^{-1})
d_g	grain diameter (m)
d_p	particle diameter (m)
J	number of mixing cells
k_M	overall mass transfer coefficient (min^{-1} or s^{-1})
L	column length (m)
Pe	Peclet number
Q_e	entry flow rate (ml min^{-1})
Re_p	pore Reynolds number
r_p	pore radius (m)
T_{exp}	filtration time (min)
t	time (min or s)
t_i	injection time of tracer (min)
t_M	transfer time of solute between the two zones (min or s)
t_D	dispersion time (min or s)
t_m	convection time in the mobile phase (min or s)
t'_M	modified transfer time (min or s)
$\bar{t}_s$	mean residence time (min or s)
t_s	residence time (s)
u_m	apparent velocity (inlet flow rate/column section) (m s^{-1})
v	volume of solution passed through the column at time t ($Q_e t$) (cm^3)
$v_p = V$	porous volume (total volume × porosity) (cm^3)
ϵ	porosity
μ'_n	order n central moment (Eq. (2)) (min^n)
μ_n	order n moment (Eq. (1)) (min^n)
η	viscosity (Pa s)
ρ	density (kg m^{-3})

References

[1] P.V. Danckwerts, Continuous flow systems: distribution of residence times, Chem. Eng. Sci. 2 (1953) 1.

[2] J. Villermaux, Génie de la Réaction Chimique, Conception et Fonctionnement des Réacteurs, Technique et Documentation, Lavoisier, Paris, 1982.

[3] J.P. Herzig, D. Leclerc, P. Le Goff, The flow of suspensions through porous media—application to deep bed filtration Ind. Eng. Chem. 5 (1970) 28–35.

[4] C. Tien, Granular Filtration of Aerosols and Hydrosols, Butterworths, London, 1989.

[5] G. Clough, K.J. Ives, Deep bed filtration mechanisms observed with fibre optic endoscopes and CCTV, 4th World Filtration Congress, Ostend, Belgium, April, 1986.

[6] M.A. Coad, K.J. Ives, Investigation of deep bed filters using tracers, Conference on Filtration and Separation for Optimum Results, Filtration Society, London, 1981.

[7] D. Dalla-Costa, G. Nouailles-Degorce, Internal Reports, LSGC-CNRS, Nancy, 1992.

[8] E. Rodier, J.A. Dodds, Streaming current measurements for determining the zeta potential of granular particles, Part. Part. Syst. Char. 12 (1995) 198–203.

[9] M. Sardin, D. Schweich, F.J. Leif, M.T. van Genuchten, Modeling the non-equilibrium transport of linearly interacting solutes in porous media: a review, Water Resources Research 27 (1991) 2287–2307.

[10] H.K. Christenson, Non-DLVO forces between surfaces—solvation, hydration and capillary effects, J. Dispersion Science Technology 9 (2) (1988) 171–206.